A Novel Intelligent Technique for Recognition of Coke Optical Texture

Fang Zhou[1,2], Guangxue Yue[3], Jianguo Jiang[1], Peizhen Wang[2]
[1] School of Computer and Information, Hefei University of Technology, Hefei, China
[2] School of Electric and Information, Anhui University of Technology, Maanshan, China
[3] College of Mathematics and Information Engineering, JiaXing University, JiaXing, China
Email: zf7782@ahut.edu.cn

***Abstract*—The classification and recognition of the coke optical texture is one of the key elements to determine the quality and guide the production of cokes. Since the traditional methods are not so ideal in the spatial and frequency domains, a novel algorithm is proposed in this paper to bridge the gap. Firstly, the coke micrograph is decomposed by a new contourlet packet (CP) for multi-scale and multi-direction, which introduces a nonsubsampled wavelet transform and a nonsubsampled directional filter banks (NSDFB). Furthermore, an adaptively weighted 2-directonal 2-dimension PCA method is put forward to extract the feature, which not only reduce the data dimensions, but also help to obtain a set of optimal basis in decomposed sub-bands. Finally, the classes of optical texture in coke micrograph are identified according to the knowledge-based similarity measure criteria on eigenvectors of selected basis. The experimental results indicate that the proposed scheme has a higher and more stable recognition rate than the conventional methods.**

***Index Terms*—coke micrograph; optical texture; contourlet packet; NSWT; NSDFB; adaptive two-dimension PCA**

I. INTRODUCTION

Coke is the main raw material for blast furnace iron-making. The optical texture observed with polarized light optical microscope is one of the most relevant characteristics of coke, because it is closely related to conductivity, thermal expansion, mechanical strength etc. [1-2]. However, the chemical industry has been, for a long time, dependent upon human expertise for classification, grading, differentiating and discriminating different types of optical texture. Although recently, there have been some researches on microstructure of coke by image analysis methods[3-5], most of them fix on determining the coke pore structure parameters or some features of the optical texture. Precise schemes for classification and recognition are rarely seen.

By reason of the complicated porosity structure with stochastic configuration and infinite fine feature of the coke micrograph, traditional image methods have remained great challenge. Wavelet transform, for its excellent time-frequency characteristics has achieved great success in signal processing domain, but it fails to capture directional information in dimensions higher than two. So in the last decade, several "geometric" wavelets, such as ridgelet [6], curvelet [7], contourlet [8] et al., have grown in popularity, in which contourlet transform (CT) is rated as a "true" two-dimension representation, because it can provide a multi-scale and multi-direction decomposition for images, which is more suitable for catching the features that are abundant in complex contours, edges, textures and background. However, CT does not give a further decomposition of the high frequency components, which may lose some details of image. Similar to wavelet packet, contourlet packet (CP) is a natural extension of CT. In papers [9-10], wavelet based contourlet packet transform (WBCPT) has been investigated and applied to image encoding and feature extraction, but it still does not resolve the frequency aliasing and shift-variant problems. So, in this paper, we apply a new decompose method called NS-WBCPT combined with a nonsubsampled wavelet transform (NSWT) [11] and a nonsubsampled directional filter bank (NSDFB) [12] to give a more accurate representation of coke micrograph.

However, the complexity of computation is considerable if directly using sub-bands of image to classification and recognition. Therefore, it needs to choose optimal basis and extract appropriate feature vectors after decomposition. Principal component analysis (PCA) [13] is a traditional data compression and feature extraction technique. In classical PCA method, 2D image matrices must be previously transformed into 1D image vectors, which results in great difficulties to evaluate the covariance matrix accurately and compute the eigenvectors efficiently. To overcome these defects, a new approach called 2DPCA was presented [14,15], in which an image covariance matrix can be constructed directly using the original image matrices, that leads to much less time for training and feature extraction. But, the main disadvantage of 2DPCA is that it needs many more coefficients for image representation than PCA. Therefore, 2-Directional 2DPCA technology ($(2D)^2PCA$) has been developed recently which considers the row and column directions simultaneously. $(2D)^2PCA$ can achieve the same or even higher recognition accuracy than 2DPCA, while the number of coefficients needed for image representation is much less [16]. However, it is still not the most suitable for all the sub-bands of our NS-WBCPT, because the size of every sub-band is equal to the original image. To resolve this problem, in our work, we propose an adaptive $(2D)^2PCA$ algorithm which can add an adaptive weight to each of sub-bands based on its

doi:10.4304/jsw.6.8.1476-1483

contribution to recognition rate. In this way, a small weighted sub-band will be removed so as to achieve a set of optimal basis for NS-WBCPT.

The remainder of this paper is organized as follows: In Section 2, the related technical preliminaries such as WBCPT and $(2D)^2$PCA methods are reviewed. The idea of our proposed scheme is described in Section 3. Section 4 provides the simulation results and compares the performance of the proposed scheme with other methods. Finally, some concluding remarks are presented in Section 5.

II. PRELIMINARIES

A. Wavelet-based Contourlet Packet Transform

Contourlet transform [8] is implemented by virtue of the Laplacian pyramids [17] and directional filter banks (DFB) [18] to provide the multi-scale and multi-directional decomposition, respectively. Wavelet-based contourlet packet transform (WBCPT) is in much the same way as we have wavelet packet transform [19]. That is, keeping in mind the anisotropy scaling law (the number of directions is doubled at every other wavelet levels when we refine the scales), we allow quad-tree decomposition of both low-pass and high-pass channels in wavelets and then apply the DFB to each sub-band. Fig. 1 schematically illustrates an example of WBCPT.

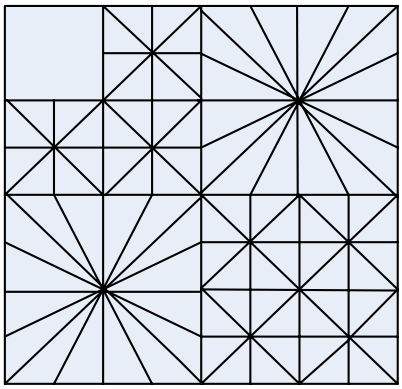

Figure 1. Schematic diagram of an example of WBCPT.

As well as known, one dimension wavelet transform can be defined as:

$$U_j^n(x) = U_{j+1}^{2n+1}(x) \oplus U_{j+1}^{2n}(x) \tag{1}$$

where

$$U_j^n(x) = U^n(x - 2^j m) \tag{2}$$

The integer j and m are the index scale and transfer operations. The index n is an operation modulation parameter or oscillation parameter. When n = 2,3,... the function can be defined by the following recursive relationships:

$$U_j^{2n}(x) = \sqrt{2}\sum_m h(m) U_{j+1}^n(2x - m) \tag{3}$$

$$U_j^{2n+1}(x) = \sqrt{2}\sum_m g(m) U_{j+1}^n(2x - m) \tag{4}$$

Where $h(m)$ and $g(m)$ are the quandrature mirror filter (QMF) associated with the scaling function and mother wavelet function. The element of corresponding space $U_j^n(x)$ is:

$$\{\psi_j^n(x - 2^j m)\}_{m \in Z} \tag{5}$$

For a two-dimension decomposition of wavelet packet, label each node of the quad-tree with a scale j, and two values p and q corresponding to the frequencies of 1D subspace. Here suppose input image with N pixels ($N^{-1/2} = 2^L$), and associate the approximation space $V_L^2 = V_L \times V_L$ to the original image. Then it has:

$$U_j^{p,q}(x,y) = U_j^p(x) \otimes U_j^q(y)$$

$$\text{Where } j - L > 0, 0 \le p < 2^{j-L}, 0 \le q < 2^{j-L} \tag{6}$$

Which satisfy $U_j^{p,q} \subset V_L^2 = U_j^{0,0}$. According to (1), the above formula can be expanded as:

$$U_j^{p,q} = U_{j+1}^{2p,2q} \oplus U_{j+1}^{2p,2q+1} \oplus U_{j+1}^{2p+1,2q} \oplus U_{j+1}^{2p+1,2q+1} \tag{7}$$

They correspond to the four children subspace of quad-tree node. Now if $\{j_i, p_i, q_i\}_{1 \le i \le L}$ are the indices of terminal nodes of WPT tree, it has the following reconstruction equation:

$$U_j^{0,0} = \oplus_{i=1}^L U_{j_i}^{p_i,q_i} \tag{8}$$

Let $t = (x, y)$, the element of space $U_j^{p,q}$ is $\{\psi_j^{p,q}(t - 2^j m)\}_{m \in Z^2}$ and the corresponding 2D WPT bases $\{\psi_{j_i}^{p_i,q_i}(t - 2^j m)\}_{m \in Z^2, 1 \le i \le L}$ construct an orthogonal basis of $V_L^2 = W_j^{0,0}$.

Now come to the formulation to the DFB stage and relate it to 2D WPT. For an l_d-level DFB, it can get 2^{l_d} directional sub-bands with $G_k^{(l_d)}(0 \le k \le 2^{l_d})$ equivalent synthesis filters and the overall down-sampling matrices:

$$S_k^{(l_d)} = \begin{cases} \begin{bmatrix} 2^{l_d-1} & 0 \\ 0 & 2 \end{bmatrix}, 0 \le k < 2^{l_d-1} \\ \begin{bmatrix} 2 & 0 \\ 0 & 2^{l_d-1} \end{bmatrix}, 2^{l_d-1} \le k < 2^{l_d} \end{cases} \tag{9}$$

Then $\{g_k^{(l_d)}[t - S_k^{l_d} m]\}(0 \le k \le 2^{l_d}, m \in Z^2)$ construct a directional basis for $L^2(Z^2)$, where $g_k^{(l_d)}$ is the impulse response of the synthesis filter $G_k^{(l_d)}$, t is the spatial index, and m is a shift in position. Now, if applying l_d directional levels to the space $U_{j_i}^{p_i,q_i}$ at a terminal node, where $p_i + q_i \ne 0$, we can obtain 2^{l_d} directional sub-bands for $U_{j_i}^{p_i,q_i}$:

$$U_{j_i}^{p_i,q_i} = \oplus_{k=0}^{2^{l_d}-1} U_{j_i,k}^{p_i,q_i(l_d)} \tag{10}$$

Using a similar proof as one provided in [20], we can show that the follow family form an orthogonal basis of $V_L^2 = W_j^{0,0}$:

$$\eta_{j_i,k,n}^{p_i,q_i,(l_d)} = \sum_{m\in Z^2} g_k^{(l_d)}[m - S_k^{l_d} n]\psi_{j_i,m}^{p_i,q_i}$$

$$\text{Where} \quad n \in Z^2, 0 \le k \le 2^{l_d}, 1 \le j \le L \tag{11}$$

B. Two-directional 2DPCA Algorithm ((2D)^{2}PCA)

Suppose A denote $m\times n$ image matrix and X denote an n-dimensional unitary column vector. The idea of 2DPCA is to project image A onto X by $Y = AX$ [13]. Then obtain an m-dimensional projected vector Y, which is called the projected feature vector of image A. In fact, 2DPCA tries to seek optimal discriminating vectors maximizing the following criterion given by:

$$\begin{aligned} J(X) &= trace(S_x) \\ &= trace\{E[(Y-EY)(Y-EY)^T]\} \\ &= trace\{E(AX-E(AX))(AX-E(AX)^T]\} \\ &= X^T E[(A-EA)^T(A-EA)]X \end{aligned} \tag{12}$$

where S_X denotes the total covariance matrix of projected samples A_i (i=1,2...M) and E is the expectation of a stochastic variable. Define the image scatter matrix G as follow:

$$G = E[(A-EA)^T(A-EA)] \tag{13}$$

Suppose there are M training images and the average image is $\overline{A}$, G can be evaluated by

$$G = \frac{1}{M}\sum_{k=1}^{M}(A_k - \overline{A})^T(A_k - \overline{A}) \tag{14}$$

Alternatively, the criterion in (12) can be rewritten as:

$$J(X) = trace(S_x) = X^T G X \tag{15}$$

It has been proven that the optimal value for the projection matrix X_{opt} is composed by orthogonal eigenvectors $X_1,X_2,\ldots X_d$ of G corresponding to the d largest eigenvalues, where $d<n$ and $X_i^T X_j = 0, i \ne j, 1 \le i, j \le d$.

As above represented, 2DPCA only learns an optimal matrix X from a set of training samplers reflecting information between rows of images, and then projects an $m\times n$ image A onto X, yielding an $m\times d$ matrix Y. However, 2-directional 2DPCA algorithm [16], uses two covariance matrices corresponding row and column respectively to gain a linear transform matrix and reduce discrimination information in horizontal and vertical directions simultaneously. The two covariance matrices of training images can be defined as：

$$\begin{aligned} G_C &= \frac{1}{M}\sum_{k=1}^{M}(A_k - \overline{A})^T(A_k - \overline{A}) \\ G_R &= \frac{1}{M}\sum_{k=1}^{M}(A_k - \overline{A})(A_k - \overline{A})^T \end{aligned} \tag{16}$$

The eigenvectors and eigenvalues of G_C and G_R can be produced from:

$$\begin{aligned} G_C \Psi_C &= \Psi_C \Lambda_C \\ G_R \Psi_R &= \Psi_R \Lambda_R \end{aligned} \tag{17}$$

Projecting an $m\times n$ image A onto Ψ_C and Ψ_R at the same time, it can yield a $q\times d$ matrix C ($q<m$ and $d<n$):

$$C = \Psi_C^T A \Psi_R \tag{18}$$

The matrix C is called the character matrix in image representation, which can be used to reconstruct the original image by

$$\hat{A} = \Psi_C C \Psi_R^T \tag{19}$$

III. PROPOSED SCHEME

In our work, we propose a novel and robust scheme for coke optical texture recognition based on improvements and integration of the two methods as mentioned in section 2. There are three main steps: (1) decompose training images into sub-bands by virtue of novel NS-WBCPT and project onto feature sub-patterns; (2) compute adaptive weight for each sub-pattern and select a set of optimal basis according to the contributions to image recognition, and (3) classify an unknown micrograph.

A. Image Decomposition

Based on multi-sampled rate theory, down-sample on filtered image may result in low-pass and high-pass frequency aliasing. Furthermore, discrete wavelet transform (DWT) lacks scale and shift-invariant features. Hence, we adopt a nonsubsampled wavelet transform (NSWT) method substitute the DWT in WBCPT.

The NSWT method can be described as follows: at each level, when the high-pass and low-pass filters are applied to the data, the two new sequences have the same length as the original sequences. To do this, the original data is not decimated while the filters at each level are modified by padding them out with zeros.

To 1D signal, the discrete approximation and detail coefficients using NSWT can be gained as [21]

$$\begin{aligned} c_{j+1,k} &= \sum_l h(l) c_{j,k+2^j l} \\ d_{j+1,k} &= \sum_l g(l) c_{j,k+2^j l} \end{aligned} \tag{20}$$

The functions $h(n)$ and $g(n)$ are, respectively, the impulse responses of low-pass and high-pass paraunitary quadrature mirror filters (QMFs) [22].

For a 2D image, separate the variables x and y, we gain the coefficients of LL, HL, LH, and HH:

$$\begin{cases} c_{j+1}(k_x,k_y) = \sum_l h(l_x)h(l_y)c_{j,k+2^j l}(l_x,l_y) \\ d^1{}_{j+1}(k_x,k_y) = \sum_l g(l_x)h(l_y)c_{j,k+2^j l}(l_x,l_y) \\ d^2{}_{j+1}(k_x,k_y) = \sum_l h(l_x)g(l_y)c_{j,k+2^j l}(l_x,l_y) \\ d^3{}_{j+1}(k_x,k_y) = \sum_l g(l_x)g(l_y)c_{j,k+2^j l}(l_x,l_y) \end{cases} \tag{21}$$

Besides, in the design of directional filter banks (DFB), the translation invariant directional expansion is not obtained because of existing down-samplers and up-samplers. So nonsubsampled directional filter banks (NSDFB) are introduced in our work, which is constructed by eliminating the down-samplers and up-

samplers in the DFB tree structure and up-sampling the filters accordingly. The up-sampling is based on the quincunx lattice, in which an image consisting of rectangular lattices was split into the round and square dot subsets. The adopted scale factor with rotated ability is as follows:

$$S = \begin{bmatrix} 1 & 1 \\ 1 & -1 \end{bmatrix} \tag{22}$$

The change of before and after quincunx interpolation is shown in Fig.2:

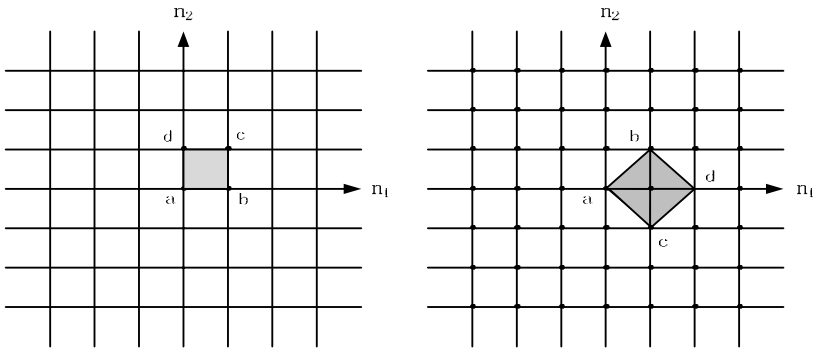

(a) Before upsampling (b) After upsampling

Figure 2. Quincunx upsample

Where *a*, *b*, *c* and *d* are the four sampled points. The correlation of interpolation results before and after is given as follows:

$$y(n_1, n_2) = \begin{cases} x(\frac{n_1 + n_2}{2}, \frac{n_1 - n_2}{2}), & n_1, n_2 \in even \\ 0, & otherelse \end{cases} \tag{23}$$

Make use of the improved algorithm with NSWT and NSDFB, a coke optical texture micrograph can be decomposed to *L* equally sub-band, whose size is *m*×*n*, as same as the original image. Fig.3 shows the decomposition process. Then project each sub-band onto *q*×*d* feature sub-pattern using 2-directioanl 2DPCA method as mentioned in section 2.2 and concatenate the *L* sub-patterns into corresponding column vectors.

The corresponding *z* transform is denoted as (24), the detail proof can confer to paper [23].

$$Y(z_1, z_2) = X(z_1, z_2, z_1 z_2^{-1}) \tag{24}$$

Suppose that there are *N* *m*×*n* original micrographs belonging to *M* categories in the training set, each category has $N_1, N_2, \ldots N_M$ micrographs respectively. $N = N_1 + N_2 + \ldots + N_M$. We collect all the vectors at the same position of all the samples to form a specific sub-pattern's training set, in this way, *L* separate sub-pattern sets are formed. This process is illustrated in Fig. 4.

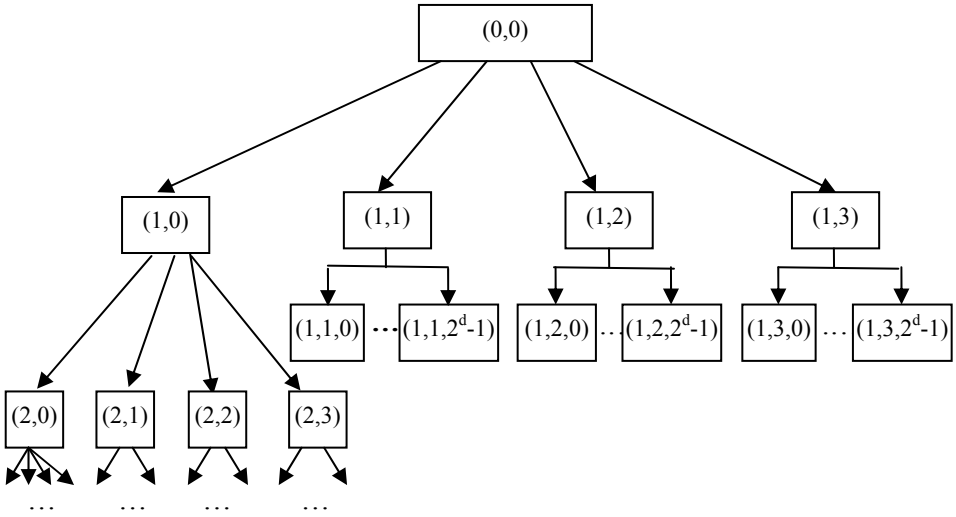

Figure 3. Diagram of decomposition process of NS-WBCPT

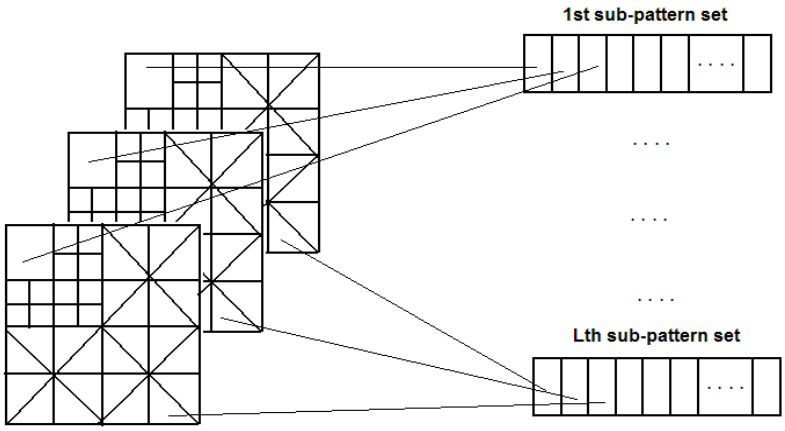

Figure 4. Image sub-pattern training sets

It should be noted that the left part of Fig.4 only indicates the decomposition level and position of NS-WBCPT sub-patterns, not reflecting the size.

B. Selection of Optimal Basis

Firstly, we construct a group of virtual samples which are generated by both the sub-pattern mean and median values of each category in sub-pattern's training set. The reason why we construct virtual samples is to use these sub-pattern representatives to determine contributions made by different parts to classification. The process of computing the contributions consists of the three following steps. In the first step, we compute sub-pattern median and mean values and define a similarity between two samples; the second step is to assign weight for each sub-pattern by computing its contributions and in the last step, we select a set of optimal and adaptively weighted sub-pattern basis according to an appreciated threshold.

Step1: For the *j*th sub-pattern, median value of the *i*th category is computed by

$$X_{ij\_median} = Median(X_{ij1}, X_{ji2}, ...X_{jiN_i}) \tag{25}$$

Similarly, the mean value by

$$X_{ij\_mean} = \frac{1}{N_i}\sum_{k=1}^{N_i} X_{ijk} \tag{26}$$

where X_{ijk} denotes the *j*th sub-pattern in the *k*th image of the *i*th category. The similarity between sub-pattern samples *X* and *Y* is defined as

$$similarity(X,Y) = \frac{\langle X,Y\rangle}{\|X\|^2 + \|Y\|^2 - \langle X,Y\rangle} \tag{27}$$

Step 2: The contribution of *j*th sub-pattern is computed as follows: Firstly, compute the similarities between a virtual sample of the *j*th sub-pattern and each sample of this sub-pattern in all the training set with all the categories. Then the training samples are ranked in the descending order of the obtained similarities, and the identity of the top 1 sample in the rank list is considered as the recognition result. If the identity and the virtual sample identity are matched, record it "true", else "false". After completing all the computation for all the virtual samples of the *j*th sub-pattern, we denote the numbers of how many virtual samples are correctly classified by C_j. Finally, we gain the contributions and weights of the *j*th sub-pattern to recognition given by

$$W_j = \frac{C_j}{2M} \tag{28}$$

Step 3: Select a set of optimal basis by setting an appreciated threshold θ and modifying the weights of all the sub-pattern as

$$W_j = \begin{cases} 0, W_j < \theta \\ W_j, W_j \ge \theta \end{cases} \quad 1 \le j \le L \tag{29}$$

C. Recognition of Test Samples

In order to classify an unknown test image *B*, the image is also first decomposed into *L* sub-bands in the same way previously applied to the training images. Then according to the optimal basis, remain *D* (*D*<*L*) sub-bands and project each of them into feature sub-pattern. The average similarity between the *j*th sub-pattern of image *B* (Y_j) and relevant ones in the *k*th image of the *i*th category in training set ($X_{j,i,k}$) , is computed as [24]:

$$\overline{S}_j(i) = \frac{1}{N_i}\sum_{k=1}^{N_i} \frac{\langle Y_j, X_{j,i,k}\rangle}{\|Y_j\|^2 + \|X_{j,i,k}\|^2 - \langle Y_j, X_{j,i,k}\rangle}, 1 \le i \le M \tag{30}$$

In this way, combing the similarities of these *D* sub-patterns and the corresponding weights W_j, the identity belonging to the *i*th category can be achieved:

$$S(i) = \sum_{j=1}^{D} W_j \cdot \overline{S}_j(i) \tag{31}$$

Finally, the category of test image *B* can be determined by following formula:

$$Class(B) = \arg\max_i (S(i)); 1 \le i \le M \tag{32}$$

IV. SIMULATION RESULTS AND ANALYSIS

In this section, we firstly construct two sample databases by the guidance of experienced experts of coke, and then evaluate the efficiency and robustness of our proposed scheme based on the two sample databases, which are called DA and DB, respectively.

A. Image Acquisition and Preprocessing

Image acquisition system of coke optical texture includes photometer, automatic scanning stage, microscope focusing system, control system, the camera above microscope eyepiece and PC, etc. The main function concentrated in a dedicated HD-type micro-photometer, such as shown in Fig. 5.

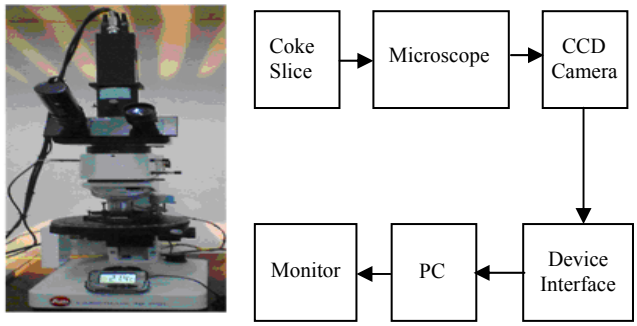

Figure 5. HD-type micro-photometer and image acquisition process

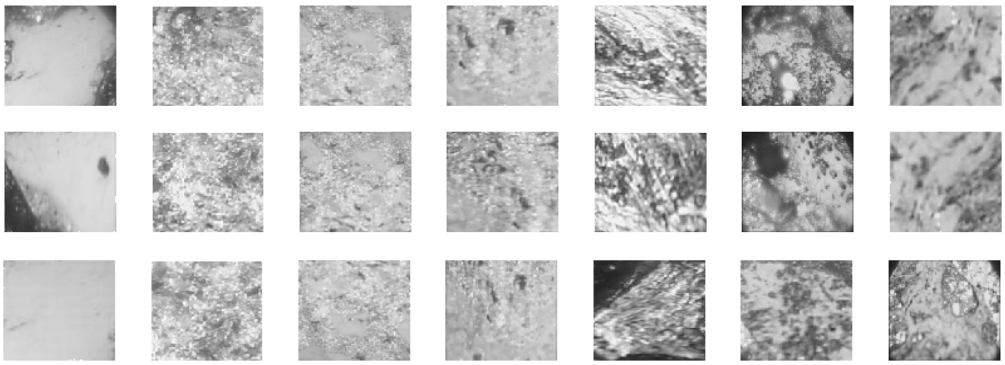

Figure 6. Three group of samples of 7 categories in database DA

There are two major categories of coke optical texture, namely the isotropic and anisotropic. Yet, the latter in turn consists of six types: they are fibrous, sheet, fragmentized, and studded, etc. Therefore, the total numbers of categories to be recognized in our experiments are seven. The following experiments are carried on PC with 1.4GHz CPU and 512MB memory and programmed in the MATLAB language.

B. Experiments on DA

In database DA, all of micrographs come from the same batch of coke samples and have the same illumination intensity. We selected 112 samples with 7 categories and every category has 16 ones, in which two-thirds as a training set, and the remaining one-third as test set. In the preprocessing step, the images are cropped and resized to a size of 128×128 pixels with 256 gray levels. Fig.6 depicts some sample images in the database DA.

The performances of the proposed method are compared with five benchmark approaches, i.e. LBP (local binary pattern) [25] which is a global algorithm widely used in space domain, WT (wavelet transform), CT [20] (contourlet transform), WPT [19] (wavelet packet transform), and WBCPT (wavelet-based contourlet packet transform) [9]. The extraction of feature sub-patterns in all of the five methods are used the algorithm $(2D)^2PCA$. Table 1 gives the results on directions of decomposition, the numbers of sub-pattern basis, recognition rate and recognition time, where parameters are set as: J=3, θ=0.45, and q=d=4. It should to be noted that all the experiment results in this section have been obtained using 20 runs in order to obtain statistically meaningful average values.

TABLE I
RESULTS OF COMPARISON WITH DIFFERENT METHODS ON DATABASE DA

Method	Directions of decomposition	Numbers of basis	Recognition rate (%)	Recognition time (s)
LBP	1	1	56.25	0.21
WT	[1,1,1]	10	82.14	0.32
CT	[8,4,4]	17	86.61	0.34
WPT	[4,4,1]	28	87.50	0.42
WBCPT	[8,4,1]	40	91.07	0.59
Our method	[8,4,1]	22	93.75	0.37

From the table, we can see that our proposed method achieves much higher recognition accuracy than the other approaches, while needs less time than WPT and WBCPT algorithms. That is because nonsubsampled WT and nonsubsampled DFB are introduced in our method, which get rid of the frequency aliasing and enhance the directional selectivity and shift-invariance property. Furthermore, by virtual of adaptively weighted method, we gain a set of optimal sub-pattern basis, which lead to

the numbers of basis in our method much less than WPT and WBCPT.

To test the noise sensitivity of different algorithms, we manually adding different density of Gaussian noise and Salt & Pepper noise into the samples of database DA. Results of comparison are shown in Fig. 7(a) and (b).

C. Experiments on DB

In database DB, most of micrographs come from different batches of coke with different illumination intensity. Similar to database DA, there are 112 samples consist of 7 categories, in which two-thirds as a training set, and the remaining one-third as test set. The images are also cropped and resized to a size of 128×128 pixels with 256 gray levels. Some of sample images in the database DB are shown in Fig.8.

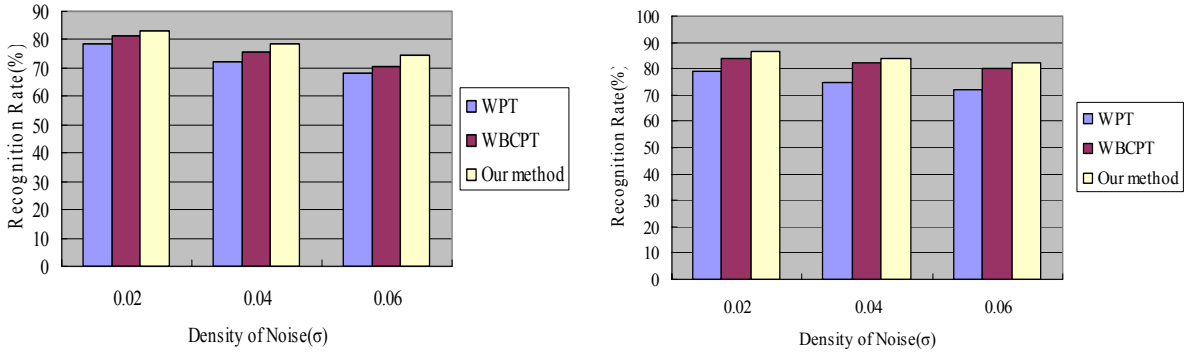

(a) Gaussian Noise (b) Salt &Pepper Noise

Figure 7. Different recognition rates under different noise

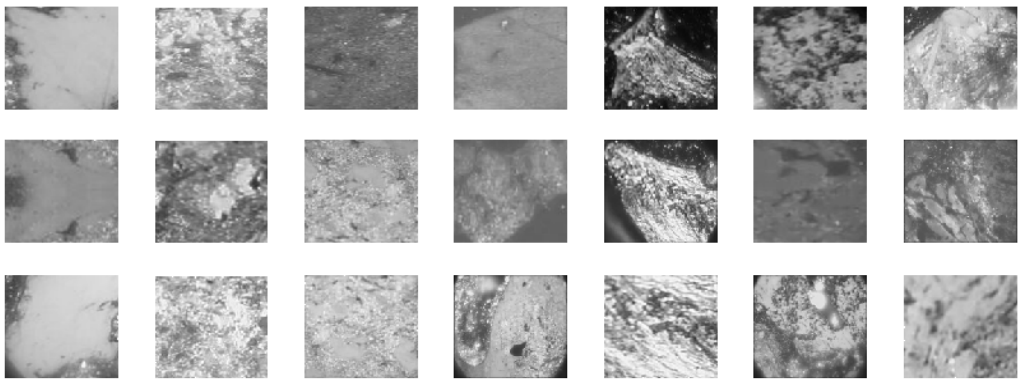

Figure 8. Three group of samples of 7 categories in database DB

Table 2 gives the comparisons of three methods where parameters are set as: J=3, t=0.3, and q=d=5. Also, our method outperforms the other methods in both accuracy and speed. Thus, our proposed method is more efficient and robust to a variety of collected samples.

TABLE II
RESULTS OF COMPARISON OF DIFFERENT METHODS ON DATABASE DB

Method	Directions of decomposition	Numbers of basis	Recognition rate (%)	Recognition time (s)
WPT	[4,4,1]	28	79.46	0.48
WBCPT	[8,4,1]	40	83.04	0.62
Our method	[8,4,1]	27	85.71	0.48

V. CONCLUSIONS

This paper presents the development and evaluation of a new tool for visual and intelligent identification of coke optical texture. By combing the finer approximation characteristic of nonsubsampled wavelet transform with the invertible characteristic of nonsubsamples directional filter banks, the image description become more precise and accurate, which is quite beneficial to subsequent identification. Furthermore, an adaptively weighted 2-directional 2-dimension PCA algorithm is employed to make decisions on extracting feature vectors and optimal basis, which not only improve the recognition accuracy, but also reduce the computational complexity at the same

time. The results of some experiments validate the efficiency and robustness.

ACKNOWLEDGMENT

The authors would like to thank the anonymous referees for their help comments and suggestions. The work was supported by the National Science Foundation of China under grant No.50874001 and No.51007002, the China Education Department Ph.D. Foundation under grant No. 20060359004, the Natural Science Foundation of Zhejiang province under grant No.Y1080901 and the Young Teacher Scientific Research Foundation of Anhui University of Technology under grant No. QZ201013.

REFERENCES

[1] H.Marsh, M.M. Escandell, F.R. Reinoso, *Carbon*, vol.37, pp.363-390, 1999.
[2] Q.L Lin, T.H Li, C.Z Zheng, Y Zhao, S.H Song, "Carbonization behavior of coal-tar pitch modified with divinylbenzene and optical texture of resultant semi-cokes", *J. Journal of Analytical and Applied Pyrolysis*, vol.71, No.2, pp 817-826, 2004.
[3] A.H. Reed, R.B. Pandey, and D.L. Lavoie, "Fractal Dimensionality of Pore and Grain Volume of a Siliciclastic Marine Sand", *International Journal of Modern Physics*, vol.11, No.8, pp.1555-1557, 2000.
[4] D.L. Zhang, "Study on Determination of Coke Pore Structure by Image Analysis", *J. Fuel & Chemical Processes*, vol.34, No.4, pp.175-178. 2003.
[5] P.Z. Wang, X.Q. Mao, X.F. Mao, F. Zhou, "Coke Photomicrograph Segmentation Based on an Improved Mean Shift Method", 2009 Asia-Pacific Conference on Information Processing, Shenzhen, China, July, 2009.
[6] M.N. Do, M. Vetterli, "The finite ridgelet transform for image representation", *J. IEEE Transactions on Image Processing* vol. 2, No.1, pp.16 – 28. 2003.
[7] J.L. Starck, E. Candès, D.L. Donoho, "The curvelet transform for image denoising", *J. IEEE Transactions on Image Processing*. vol. 11, No.6, pp. 670-684. 2002.
[8] M.N. Do, M. Vetterli, The contourlet transform: an efficient directional multi-resolution image representation, *IEEE Transactions on Image Processing*, vol. 14, No. 12, pp. 2091-2106. 2005.
[9] R. Eslami, H. Radha, "Wavelet-based contourlet packet image coding", in the Conference on Information Sciences and Systems, The Johns Hopkins University, March 2005.
[10] S.Y Yang, M. Wang, L.C Jiao, "Radar target recognition using contourlet packet transform and neural network approach", *J. Signal Processing*, vol.89, NO.4. pp. 394-409, 2009.
[11] J.L. Starck, J. Fadili, and F. Murtagh, "The undecimated wavelet decomposition and its reconstruction", *J. IEEE Transactions on Image Processing*, vol.16, No.2 pp. 297-309, 2007.
[12] A.L. Cunha, J.P. Zhou, and M.N. Do, "The nonsubsampled contourlet transform: theory, design, and applications", *J. IEEE Transactions on Image Processing*, vol.15, No.10 pp. 3089-3101, 2006.
[13] I.T. Jolliffe, *Principal Component Analysis*, Springer-Verlag, New York, 1986
[14] J. Yang, D. Zhang, A.F. Frangi, and J.Y. Yang, "Two-dimensional PCA: a new approach to appearance-based face representation and recognition," *J. IEEE Trans. on Pattern Analysis and Machine Intelligence*, vol. 26, no. 1, pp. 131-137, Jan. 2004.
[15] D.Q. Zhang, S.C. Chen, and J. Liu, "Representing image matrices: Eigenimages vs. Eigenvectors", In the Proceedings of the 2nd International Symposium on Neural Networks (ISNN'05), Chongqing, China, vol. 2, pp. 659-664, 2005.
[16] T.Y, J.H Ahn, Y.G Kim, Y.J Song, U.D Chang, D.W Kim, "Face recognition using a fusion method based on bidirectional 2DPCA", *J. Applied Mathematics and Computation*, vol.20, No.5, pp.601 – 607, 2008.
[17] P.J. Burt, E.H. Adelson, "The Laplacian pyramid as a compact image code", *J. IEEE Transactions on Communication*, vol.31, No.4, pp.532~540. 1983.
[18] Y.M Lu, M.N. Do, "Multidimensional Directional Filter Banks and Surfacelets", *J. IEEE Transaction on image processing*, Vol. 16, N0. 4, pp. 918-931. 2007.
[19] F. G. Mayer, A. Z. Averbuch, and J.-O. Stromberg, "Fast adaptive wavelet packet image compression," *J.IEEE Trans. Image Processing*, vol. 9, no. 5, pp. 792-800, May 2000.
[20] M.N. Do and M. Vetterli, "Contourlets," in *Beyond Wavelets*, Academic Press, New York, 2003
[21] H.L. X, T.X. Zhang, and Y.S. Moon, "A Translation- and Scale-Invariant Adaptive Wavelet Transform", *J. IEEE Trans. Image Processing*, vol. 9, no. 12, pp. 2100-2108, 2000.
[22] J.D. Wu, C.H Liu, "An expert system for fault diagnosis in internal combustion engines using wavelet packet transform and neural network", *J. Expert Systems with Applications*, vol. 36, No.3, pp. 4278-4286. 2009.
[23] F. S. Yang. *Project Analysis and Application of Wavelet Transform*. Beijing, Scientific Press, pp. 121-126, 1999.
[24] A. Chao, R.L. Chazdon, R.K. Colwell and T.J. Shen, "A new statistical approach for assessing similarity of species composition with incidence and abundance data", *J. Ecology Letters*, Vol. 8, pp.148–159. 2005
[25] T. Ahonen, A. Hadid, M. Pietikainen, "Face recognition with local binary patterns". In the proceedings of the 8th European Conference on Computer vision (ECCV), Prague, Czech Republic, pp.469~481. May 2004.

Fang Zhou received her B.S. degree and M.S. degree both major at Electric Engineering from Anhui University of Technology, Maanshan, China in 1999 and 2004, respectively. From September 2007, she is a Ph.D. candidate in Hefei University of Technology. At the same time, she is an Associate Professor in Anhui University of Technology. Her research interests are in the area of signal processing and pattern recognition, in particular, the application of digital image processing technology in the metallurgical industry. E-mail: zf7782@ahut.edu.cn